2024 IEEE Symposium on VLSI Technology and Circuits (VLSI Technology and Circuits) | 979-8-3503-6146-9/24/$31.00 ©2024 IEEE | DOI: 10.1109/VLSITECHNOLOGYANDCIR46783.2024.10631318

Unveiling Cryogenic Performance (4 to 300 K) towards Ultra-thin Ferroelectric HZO: Novel Kinetic Barrier Engineering and Underlying Mechanism

Dong Zhang[1†], Yang Feng[1,2†], Zijie Zheng[1], Chen Sun[1], Qiwen Kong[1], Gan Liu[1], Zuopu Zhou[1],
Gengchiau Liang[1,3], Kai Ni[4], Jixuan Wu[2]*, Jiezhi Chen[2*], and Xiao Gong[1*]
[1]ECE, National University of Singapore, Singapore, Singapore; [2] School of Information Science and Engineering, Shandong University, Qingdao, China;
[3]Industry Academia Innovation School, National Yang-Ming Chiao Tung University, Hsinchu City, Taiwan; [4]University of Notre Dame, IN, USA.
[†]Equally contributing authors; [*]Email: jixuanwu@sdu.edu.cn, chen.jiezhi@sdu.edu.cn, elegong@nus.edu.sg

Abstract- We perform comprehensive and in-depth investigation into the cryogenic characteristics of ferroelectric (FE) HZO thin films with varying thicknesses (3/5/7/10 nm) across a broad temperature range (4~300 K), assisted by the first-principles calculations as well as extensive material and electrical characterizations. We discover: (1) 3 and 5 nm HZO films exhibit distinct temperature dependence in remnant polarization (P_r) and coercive field (E_c) as compared with 7 and 10 nm ones owning to different phase transition mechanisms. (2) The concentration and location of V_o^{2+} emerge as pivotal factors influencing the trap-assisted-tunneling process, and thereby the temperature-dependent behaviors of P_r and E_c. (3) V_o^{2+} possesses a lower migration energy barrier as compared with V_o, and oxygen vacancy concentration can be engineered through O_3 pulse duration during ALD deposition of HZO. Building upon these insights, we propose and experimentally demonstrated, for the first time, an innovative cryogenic barrier engineering approach for P_r enhancement, particularly valuable for ultra-thin HZO films.

I. Introduction

The immense potential of HfO_2-based FE memories for storage and computing have been showcased through their remarkable progress in recent years [1]. Continuous advancements require further simultaneous reduction in operating voltage and enhancement in integration density, both vertically and horizontally. FE thickness down-scaling emerges as one of the most promising and cost-effective approaches. While ferroelectricity in ultra-thin HZO films has been reported, it typically comes with the caveat of drastic performance degradation [2]. Furthermore, the dynamic landscape of emerging technologies and applications adds on exciting dimension to the exploration of ferroelectric devices at cryogenic temperatures, i.e. data center and quantum computing. This calls for a more comprehensive and in-depth understanding of cryogenic ferroelectric behaviors across a broad temperature range, despite some recent reports in this domain [3-6].

This study delves into the FE behavior of HZO with thickness as thin as 3 nm and temperatures spanning from 4 K to 300 K. Our in-depth investigation unveils a comprehensive understanding of ferroelectric cryogenic mechanisms involving phase transition, oxygen vacancy (V_o^{2+}), the dead layer, and traps. This enables us to pioneer a novel cryogenic wake-up strategy tailed to enhance FE properties, particularly critical for ultra-scaled FE film thickness, i.e. <3 nm. The findings of work offer valuable insights for advancing process optimization and refining device design, applicable to a diverse spectrum of FE applications. Motivations of our work are summarized in Fig. 1, with key contributions highlighted in Fig. 2 (a).

II. Cryogenic performance and analysis of HZO

A. Temperature dependence of P_r and E_r with different HZO Thicknesses

Fig. 2 (b) shows the key process skeps for fabricating HZO capacitors. Fig. 2 (c) gives cross-sectional TEM images of a 3 nm HZO capacitor with a clear dead layer. To investigate the behaviors and mechanisms of cryogenic HZO performance, P-V curves for capacitors with different HZO thicknesses (3 to 10 nm) at various temperatures (4 K to 300 K) are plotted in Fig. 3. As summarized in Fig. 4 (a), for 3 nm and 5 nm HZO, P_r increases as test temperature decreases, while 7 nm and 10 nm HZO give opposite trend. Fig. 4 (b) further illustrates the behavior of the E_c, showing a declining trend with lower temperatures for 3 nm HZO and an augmented E_c at lower temperatures for 7 nm and 10 nm HZO.

B. The role of oxygen vacancy and the dead layer (7 nm and 10 nm)

To delve into the underlying mechanisms governing these contrasting changes, we initiated an oxygen vacancy analysis for 7 nm and 10 nm HZO capacitors. For pristine HZO, the V_o^{2+} is primarily concentrated at the bottom electrode (BE) (Fig. 5), and will redistribute under electric cycling. We perform 10^3 cycles of the electrical field (~3.5 MV/cm) at 300 K to induce the redistribution of V_o^{2+}, and the corresponding FE characteristics are depicted in Fig. 6. We found: (1) after redistribution of the oxygen vacancy, P_r stabilizes with varying temperatures, suggesting that the Vo^{2+} could be the primary reason of P_r reduction for 7 and 10 nm HZO capacitors at cryogenic temperatures. (2) Electrical cycling introduces more significant change in E_c as temp. reduces from 300 K to 4 K over pristine state without cycling.

Frequency test was further carried out and results (Fig. 7). Interestingly, E_c of 7 nm and 10 nm HZO exhibits strong frequency dependence at 77 K and 300 K for both the pristine device and device with cycling, suggesting a strong correlation between E_c increase and the trap effects. In addition, the more pronounced E_c increase after V_o^{2+} redistribution suggests a high likelihood of influence from the traps located near the BE [8]. This can be explained by the fact that, after oxygen vacancy redistribution, the probability of trap-assisted tunneling (TAT) reduces and the temperature dependence is more obvious (Fig. 8). These observations can be substantiated by the first-principles calculation results in Fig. 10 where V_o^{2+} has a much smaller migration barrier than V_o [9].

C. Temperature-dependent phase transition (3 nm)

For the ultra-thin HZO capacitors, i.e. 3 nm and below, t-phase is the dominant phase [10]. The HZO is crystalized with t-phase during high temperature process, i.e. RTA annealing. Such t-phase is difficult to transit to f-phase during the cooling down due to the high transition barrier induced by a small grain size with an ultra-thin thickness. Interestingly, as the temperature reduces, the relative free energy of t-phase is lifted up, reducing the kinetic barrier from t- to f-phase (Fig. 11). As the t phase transitions to the f phase during cycling under cryogenic temperatures, the dielectric constant of the HZO layer decreases, with the f phase exhibiting a smaller dielectric constant than the t phase. Consequently, a larger portion of the applied voltage drops across the HZO layer, leading to a reduction in apparent E_c (Fig. 9).

To clarify the impact of oxygen vacancy on P_r of ultra-thin HZO capacitor, we intentionally engineered the concentration of oxygen vacancy by adjusting the O_3 pulse duration during HZO ALD deposition (Fig. 12). It was found that shorter O_3 duration yields more extensive oxygen vacancy which hinders P_r enhancement due to a more significant pinning effect (Fig. 13).

D. Summary of temperature-dependent FE characteristics with varying HZO Thicknesses

The summary of the ferroelectric characterization and the relevant mechanism at cryogenic temperature is listed in Fig. 14. In the case of the t-phase-rich HZO capacitor (i.e., 3 nm), the observed increase in P_r is attributed to the phase transition from the t-phase to the f-phase. Simultaneously, the E_c decrease is induced by the reduction in dielectric constant of HZO layer. Conversely, for the f-phase-rich HZO capacitor (i.e., 7 nm), the P_r decreases owes to the oxygen vacancy pinning effect, and the E_c increase is due to the diminished probability of trap-assisted tunneling.

III. Cryogenic wake-up strategy (kinetic barrier engineering) for ultra-thin HZO films

As the f-phase with lower free energy at 300 K is more stable than t-phase [Fig. 15. (a)], the phase transition that happens at cryogenic temperature with electric field assistant can be maintained even after returning to 300 K. This can be substantiated by the results in Fig. 15. (b), where P_r of 3 nm HZO with kinetic barrier engineering at 4 K increases by 96% over the pristine state and the enhancement becomes more pronounced with lower kinetic barrier engineering temperatures [Fig. 15. (c)]. Furthermore, Fig. 16 indicates that endurance of HZO capacitors with all thicknesses exhibits improvement at cryogenic temperatures.

IV. Conclusions

Through comprehensive investigation into cryogenic performance of HZO, the underlying mechanisms of temperature-dependent P_r and E_c have been clarified for different HZO thicknesses. We further proposed a cryogenic wake-up strategy to achieve a substantial (96%) P_r enhancement for 3 nm HZO. Our work represents a noteworthy advancement in understanding ultra-thin HZO films, paving the way for innovative approaches to optimize FE properties across a broad temperature spectrum and offering potential applications in various fields.

Acknowledgment Acknowledgement of support from Ministry of Education (Singapore) Tier 2 Academic Research Grant (MOE-T2EP50221-0008), NSF 2346953, and China Key Research and Development Program under Grant (2023YFB4402500, 2023YFB4402400), National Natural Science Foundation of China (Nos. 62034006, U23B2040).

References [1] U. Schroeder, *et al., Nat. Rev. Mater.,* 2022; [2] Z. Gao, *et al., EDL*, 2021; [3] J. W. Adkins, *et al., APL.,* 2020; [4] C. Sun, *et al., EDL*, 2021;[5] B. Nie, *et al., EDL*, 2023; [6] M. H. Park, *et al., AEM*, 2018; [7] M. Dawber, *et al., J. Phys. Condens. Matter*, 2003; [8] S. Starschich, *et al., APL,* 2016; [9] A. Kyrtsos, *et al., Phys. Rev. B*, 2016; [10] J. Wu, *et al., APL*, 2020.

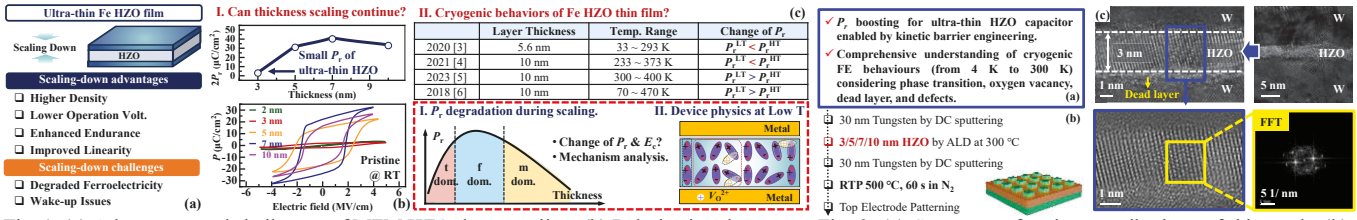

Fig. 1. (a) Advantages and challenges of MFM HZO down-scaling. (b) Polarization decreases rapidly with HZO thickness down-scaling. (c) Complex temperature-dependent FE performance requires a clearer understanding of cryogenic behaviors.

Fig. 2. (a) Summary of major contributions of this work. (b) Key process steps of FE capacitors. (c) Cross-sectional TEM images and FFT of a FE capacitor with a 3 nm-thick HZO film.

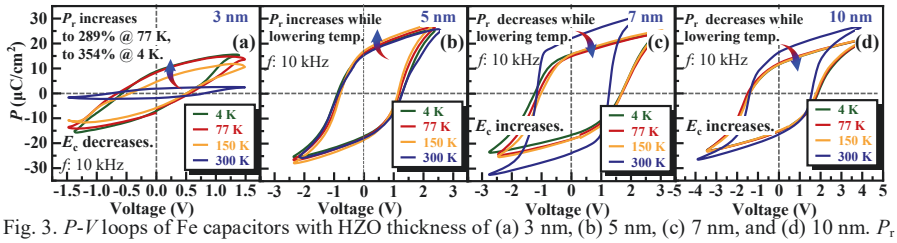

Fig. 3. *P-V* loops of Fe capacitors with HZO thickness of (a) 3 nm, (b) 5 nm, (c) 7 nm, and (d) 10 nm. P_r of the 3 nm and 5 nm devices increases as the temperature decreases. In contrast, P_r of the 7 nm and 10 nm ones decreases at lower temperatures, accompanied by noticeable changes in E_c.

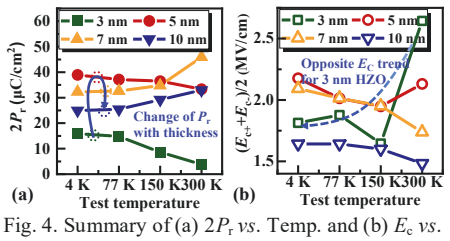

Fig. 4. Summary of (a) $2P_r$ *vs.* Temp. and (b) E_c *vs.* Temp. for various HZO thicknesses, where 3 nm HZO shows a distinct trend over 7/10 nm HZO.

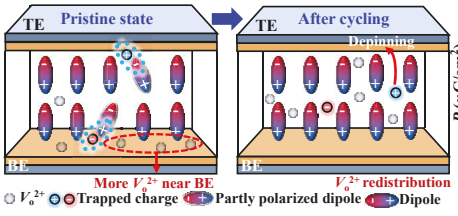

Fig. 5. After cycling, the oxygen vacancy redistributes from near the bottom electrode to the bulk HZO film.

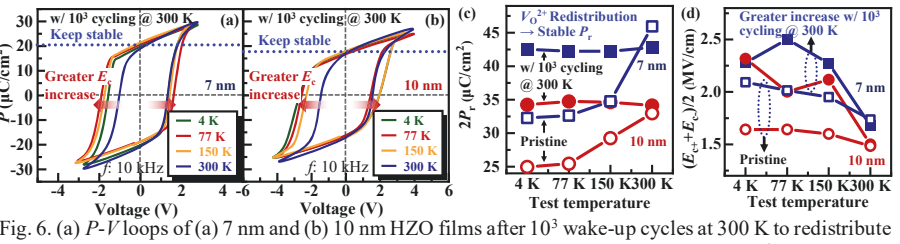

Fig. 6. (a) *P-V* loops of (a) 7 nm and (b) 10 nm HZO films after 10^3 wake-up cycles at 300 K to redistribute oxygen vacancy. The summary of (c) $2P_r$ and (d) E_c suggests that the redistribution of V_O^{2+} could be the primary reason of lower P_r in cryogenic HZO for 7 and 10 nm. E_c changes should also be related to V_O^{2+}.

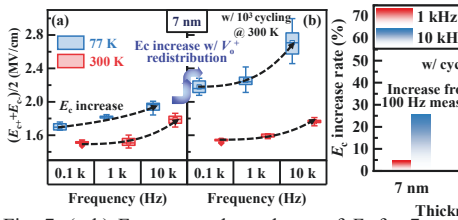

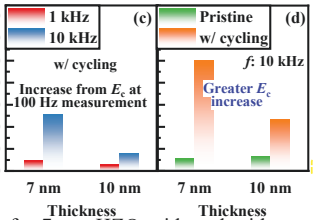

Fig. 7. (a-b) Frequency-dependence of E_c for 7 nm HZO with and without cycling at 300 K. (c-d) Summary of E_c increase rate, suggesting trap-related behaviors that are dependent on temperature and V_O^{2+} distributions.

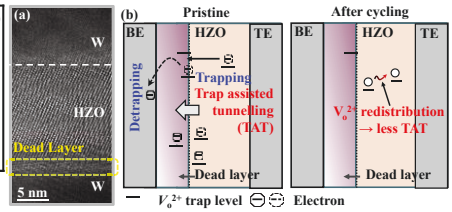

Fig. 8. (a) TEM and (b) influence of the dead layer for 10 nm HZO. With the redistribution of V_O^{2+}, the probability of TAT decreases.

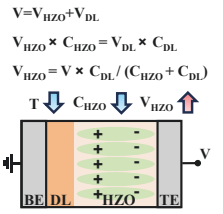

Fig. 9. Schematic shows E_c reduction induced by phase transition.

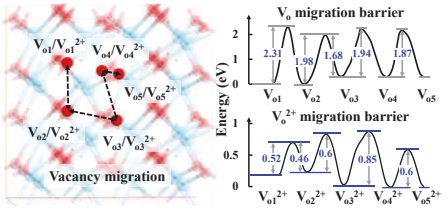

Fig. 10. The first-principles calculation results suggest a much lower energy migration barrier for V_O^{2+} as compared with V_O. The left figure illustrates the possible vacancy migration.

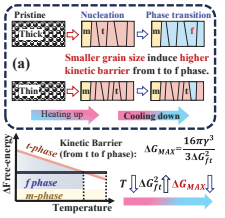

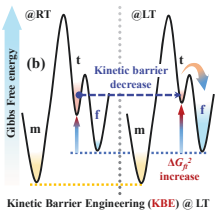

Fig. 11. (a) Cartoon showing the impact of lowering the temperature on the transition barrier from t to f phase. (b) The lower transition barrier at cryogenic enhances the probability of such a phase transition.

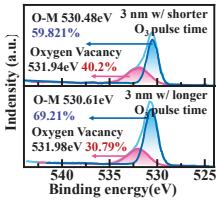

Fig. 12. Oxygen vacancy concentration can be engineered by varying O_3 pulse during ALD.

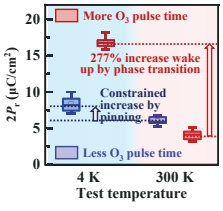

Fig. 13. Less V_O^{2+} gives a much greater increase in $2P_r$ with reducing temperature.

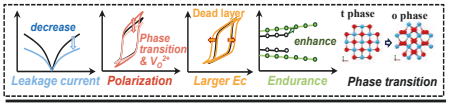

Cryogenic HZO		P_r	E_c
t-phase rich (thin)	Relation	@ LT > @ RT	@ LT < @ RT
	Mechanism	Phase transition	Phase transition
o-phase rich (thick)	Relation	@ LT < @ RT	@ LT >@ RT
	Mechanism	V_O^{2+}	Dead layer

Fig. 14. Summary of behaviors and their mechanisms of HZO at cryogenic temperature.

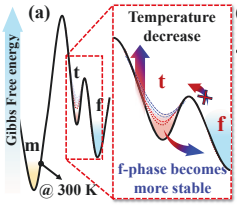

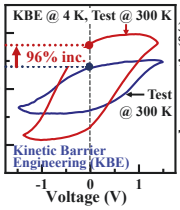

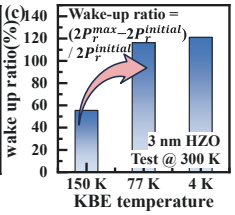

Fig. 15. (a) Higher free energy of t-phase than f-phase at 300 K indicates that the f-phase is more stable than t-phase. (b) The benefit of elevated t-phase energy during barrier engineering at 4 K with one cycle of cryogenic wake-up remains after returning to 300 K. (c) The wake-up ratio at different KBE temp.

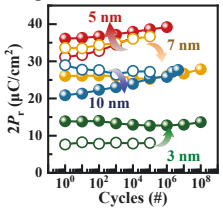

Fig. 16. Improvement in endurance at cryogenic temperature HZO with all thicknesses.